PROCEEDINGS OF SPIE

SPIEDigitalLibrary.org/conference-proceedings-of-spie

Epitaxial integration of high-performance quantum-dot lasers on silicon

Norman, Justin, Liu, Songtao, Wan, Yating, Zhang, Zeyu, Shang, Chen, et al.

Justin C. Norman, Songtao Liu, Yating Wan, Zeyu Zhang, Chen Shang, Jennifer G. Selvidge, Mario Dumont, M. J. Kennedy, Daehwan Jung, Jianan Duan, Heming Huang, Robert W. Herrick, Frederic Grillot, Arthur C. Gossard, John E. Bowers, "Epitaxial integration of high-performance quantum-dot lasers on silicon," Proc. SPIE 11285, Silicon Photonics XV, 1128504 (26 February 2020); doi: 10.1117/12.2542912

SPIE.

Event: SPIE OPTO, 2020, San Francisco, California, United States

Downloaded From: https://www.spiedigitallibrary.org/conference-proceedings-of-spie on 13 May 2020 Terms of Use: https://www.spiedigitallibrary.org/terms-of-use

Invited Paper

Epitaxial integration of high-performance quantum-dot lasers on silicon

Justin C. Norman*[a], Songtao Liu[a], Yating Wan[a], Zeyu Zhang[a], Chen Shang[a], Jennifer G. Selvidge[a], Mario Dumont[a], MJ Kennedy[a], Daehwan Jung[b], Jianan Duan[c], Heming Huang[c], Robert W. Herrick[e], Frederic Grillot[c,d], Arthur C. Gossard[a], John E. Bowers[a]

[a]University of California, Santa Barbara, Santa Barbara, California 93106, USA; [b]Center for Opto-electronic Materials and Devices, Korea Institute of Science and Technology, Seoul 02792, South Korea; [c]LTCI, Télécom Paris, Institut Polytechnique de Paris, Palaiseau 91120, France; [d]Center for high Technology Materials, 1313 Goddard SE, Albuquerque, NM87106-4343, United States; [e]Intel Corp. Santa Clara, California 95054

jnorman@ucsb.edu

ABSTRACT

Direct epitaxial growth of III-V lasers on silicon provides the most economically favorable means of photonic integration but has traditionally been hindered by poor material quality. Relative to commercialized heterogeneous integration schemes, epitaxial growth reduces complexity and increases scalability by moving to 300 mm wafer diameters. The challenges associated with the crystalline mismatch between III-Vs and Si can be overcome through optimized buffer layers including thermal cyclic annealing and metamorphic layers, which we have utilized to achieve dislocation densities $< 7\times10^{6}$ cm^{-2}. By combining low defect densities with defect-tolerant quantum dot active regions, native substrate performance levels can be achieved. Narrow ridge devices with threshold current densities as low as ~130 A/cm^2 have been demonstrated with virtually degradation free operation at 35°C over 11,000 h of continuous aging at twice the initial threshold current density (extrapolated time-to-failure >10,000,000 h). At 60°C, lasers with extrapolated time-to-failure >50,000 h have been demonstrated for >4,000 h of continuous aging. Lasers have also been investigated for their performance under optical feedback and showed no evidence of coherence collapse at back-reflection levels of 100% (minus 10% tap for measurement) due to the ultralow linewidth enhancement factor ($\alpha_H < 0.2$) and high damping of the optimized quantum dot active region.

Keywords: Quantum dot, silicon photonics, heteroepitaxy

1. INTRODUCTION

Recent years have shown rapid development and commercialization of silicon photonics for applications in datacom[1], telecom[2], and biosensing[3], and silicon photonics has positioned itself as a leading contender in future applications in LIDAR[4], neuromorphic computing[5], and quantum communications.[6] The primary driver in the adoption of silicon photonics is its comparably low cost per die relative to competing technologies through its leveraging of high yield, high throughput CMOS manufacturing technologies. Despite its imminent dominance, there is much room for further improvement in performance and manufacturability by transitioning from the hybrid and heterogeneous methods of gain integration currently being deployed to a new paradigm of direct epitaxial growth of III-V materials on silicon.[7]

Decades of research has been performed in the pursuit of high quality III-V epitaxy on silicon, but progress has been hindered by defects (i.e. dislocations, antiphase domains, and cracks) that result from the mismatch in crystal lattice between the two materials. In the last few years, extremely rapid progress has been made toward this goal through a combination of optimized III-V/Si buffers[8, 9] and defect-tolerant InAs quantum dot (QD) gain media[10-12]. By eliminating antiphase domains and reducing dislocation densities into the ~10^{6} cm^{-2} range, excellent device performance and reliability near room temperature (>10,000,000 h extrapolated time-to-failure at 35°C) have been obtained and highly promising results at elevated temperatures (>50,000 h extrapolated time-to-failure at 60°C) are currently being observed.

Fortuitously, QD lasers not only provide excellent tolerance of crystalline defects, but they also possess unique advantages for laser performance that cannot be matched by quantum wells.[13] Perhaps the most notable of these advantages are record-

Silicon Photonics XV, edited by Graham T. Reed, Andrew P. Knights, Proc. of SPIE Vol. 11285, 1128504 · © 2020 SPIE · CCC code: 0277-786X/20/$21 · doi: 10.1117/12.2542912

Downloaded From: https://www.spiedigitallibrary.org/conference-proceedings-of-spie on 13 May 2020
Terms of Use: https://www.spiedigitallibrary.org/terms-of-use

setting high temperature operation on native substrates[14], the insensitivity of quantum dot lasers to external optical feedback[15, 16] and the engineerable gain spectrum and ultrafast gain recovery that enable excellent mode-locked laser (MLL)[17] and amplifier[18] performance. Nothing precludes the transfer of these capabilities to Si substrates; in fact, the referenced MLL and amplifier performance were demonstrated in epitaxially grown QD lasers on Si.

To obtain the results referenced above and achieve the future promise of QD lasers grown on Si requires highly optimized epitaxial material stacks and growth conditions. The sections below review our progress in this area and highlight the performance gains we have obtained with improved material quality and design. One key criterion to developing these lasers into useful technologies is the ability to guide light and integrate with other optoelectronic components. We have begun to investigate this area and offer some proposed implementations and preliminary results below.

2. EPI DESIGN AND FABRICATION

There are two key, somewhat independent thrusts toward achieving high performance epitaxial lasers on silicon: III-V/Si buffer optimization to minimize the defect density and quantum dot growth optimization to increase dot density and uniformity. Optimizing the buffer layers is an exercise in the design of the epi stack to include strained layers that filter dislocations and high temperature (>700°C) thermal cycling steps to allow dislocations to move within the material and annihilate each other. Antiphase domains and other defects can be dealt with through an appropriate choice of growth template such as patterned v-grooves [19] in the Si or a GaP interlayer [20]. Optimizing the QDs is primarily based around fine tuning the growth conditions, which make up a relatively large, coupled, and highly sensitive parameter space while the surrounding material constituting the laser cavity has a relatively established set of viable designs in the literature.

We have utilized metalorganic chemical vapor deposition (MOCVD) grown GaP/Si templates purchased from NAsP$_{III/V}$, GmbH with molecular beam epitaxy (MBE) grown buffer and laser epi layers. All of the devices are fabricated using standard semiconductor fabrication techniques. The laser ridge is dry etched using an inductively coupled plasma tool. Contact and probe metallizations were deposited using electron-beam deposition. The ridges are all deeply etched through the active region with a 30 nm alumina passivation layer deposited by atomic layer deposition and a few hundred nanometer, sputtered SiO_2 isolation layer. The fabricated devices utilized two topside contacts and as-cleaved facets except as detailed below. A schematic is shown in Figure 1.

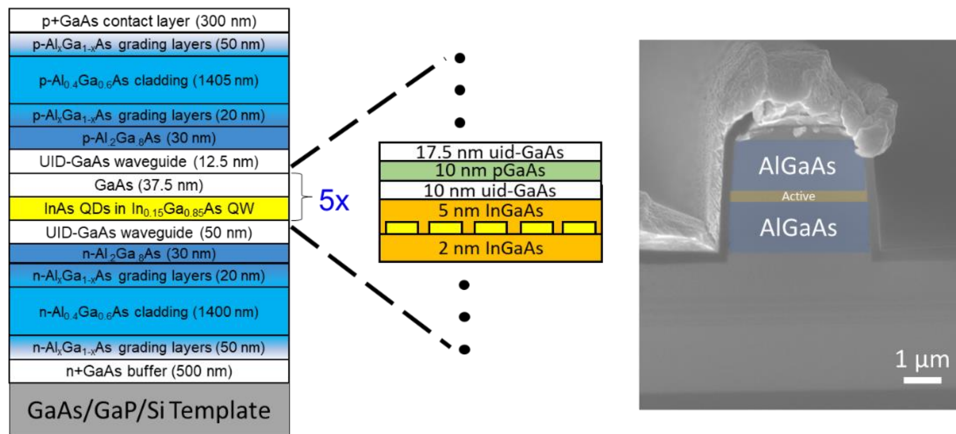

Figure 1. Schematic of the epitaxial quantum dot laser structure (left) and cross-sectional scanning electron microscope image of a cleaved laser facet (right).

Buffer designs on the GaP/Si template began with a relatively simple low temperature (~500°C) GaAs layer followed by a high temperature (~600°C) GaAs layer, resulting in a surface roughness of ~8 nm rms and a threading dislocation density of ~3×10^8 cm^{-2}. Next thermal cyclic annealing (TCA) was added through four cycles of heating to 700°C and cooling to 400°C before returning to the growth temperature of 600°C. TCA brought the dislocation density down to 7×10^7 cm^{-2}. The third step was the implementation of strained InGaAs filter layers which, with sufficient optimization, brought the dislocation density down to 7×10^6 cm^{-2} with a surface roughness of ~2 nm rms. The full details of the buffer development process are presented in [9]. Three iterations are shown in Figure 2.

Downloaded From: https://www.spiedigitallibrary.org/conference-proceedings-of-spie on 13 May 2020
Terms of Use: https://www.spiedigitallibrary.org/terms-of-use

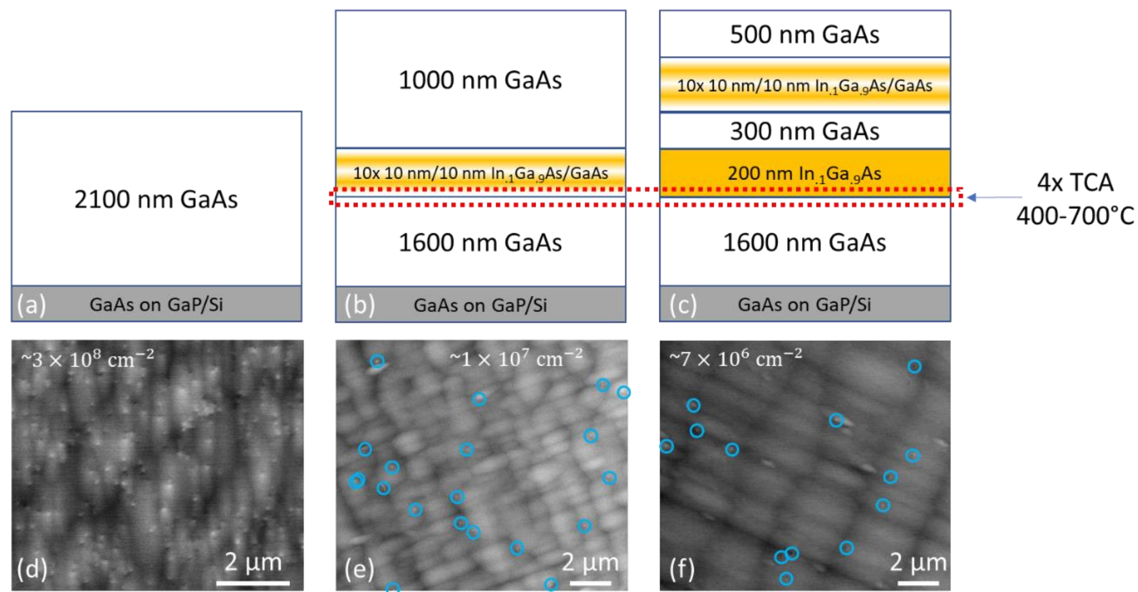

Figure 2. (a-c) Epi layer schematics corresponding to three iterations of buffer optimization beginning with (a) a simple two-step GaAs growth involving low temperature nucleation and a high temperature buffer, then (b) adding strained layer superlattices and thermal cyclic annealing (TCA), and (c) further adding a 200 nm constant composition $In_{0.1}Ga_{0.9}As$ layer. (d-f) Electron channeling contrast images illustrating threading dislocations intersecting the surface of the buffer. Dislocations in (e-f) have been circled to enhance visibility.

Quantum dot optimization pursued simultaneously high dot density with high size uniformity. QDs represent three dimensionally confined quantum structures such that their size dispersion results in an inhomogeneously broadened gain spectrum that should be minimized for optimal performance [13]. The dispersion in dot sizes results from their formation via a highly kinetically constrained self-assembly process in the Stranski-Krastanov growth regime. To minimize the inhomogeneous broadening, the coupled parameters of growth temperature, V/III flux ratio, growth rate, and total InAs deposition thickness must all be optimized along with the same space of conditions in both the InGaAs prelayer and capping layer that forms the overall dot-in-a-well (DWELL) structure. This parameter space is extremely broad and, to date, no thorough design of experiments study has been published, but various portions have been investigated with [21-24] being some of the most broad in scope. Through careful optimization, we have ultimately achieved a simultaneous quantum dot density of 6×10^{10} cm^{-2} with a photoluminescence (PL) full-width at half-maximum (a direct proxy for the inhomogeneous broadening) of 30 meV near 1300 nm.

3. LASER PERFORMANCE VS. MATERIAL QUALITY

To precisely investigate the impact of dislocation density on laser performance, three samples were fabricated with identical laser epi structures to each other: two samples grown on III-V/Si templates with threading dislocation densities of 7×10^{7} cm^{-2} and 1×10^{7} cm^{-2} and one sample grown on a native GaAs substrate. These samples differed from the epi design of Figure 1 in that they had seven dot layers. The performance of as-cleaved lasers from all three samples (1.5 mm laser cavity) is presented in Figure 3. The performance improvement between the high and low TDD templates on Si is quite substantial, particularly regarding output power and differential quantum efficiency (DQE) where improvements of a factor of ~2 can be observed at several ridge widths.

Downloaded From: https://www.spiedigitallibrary.org/conference-proceedings-of-spie on 13 May 2020
Terms of Use: https://www.spiedigitallibrary.org/terms-of-use

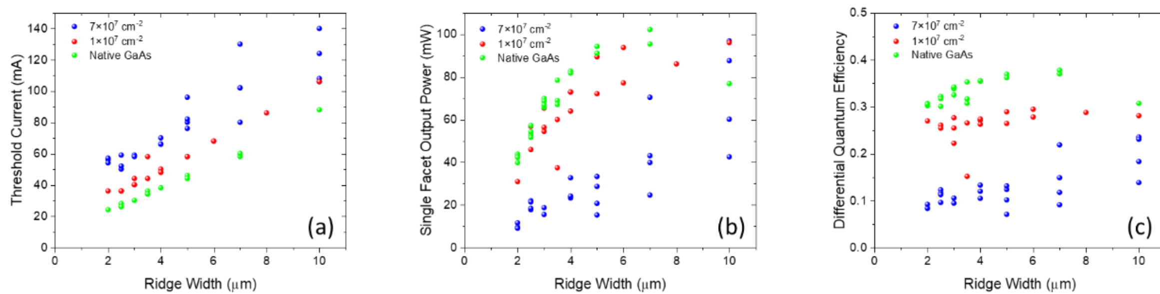

Figure 3. (a) Threshold current, (b) single facet output power, and (c) differential quantum efficiency are plotted versus ridge width for 1.5 mm as-cleaved laser cavities at varying dislocation density on silicon and for a laser grown on a native GaAs substrate with otherwise identical epi structure. These devices differ from the schematic in Figure 1 by having seven quantum dot layers.

Interestingly, the difference in performance between the low TDD sample and the laser on native substrate is much smaller. While, these are all continuous wave measurements, and the thermal conductivity of Si is much higher than GaAs, a difference in thermal impedance cannot fully explain the difference in performance because the DQE results are taken from the light output very near threshold where dissipated power is relatively low. These devices exhibit series resistances from ~1-3 Ω depending on ridge width with no systematic difference between the three samples. Diminishing returns are not unexpected as the dislocation density is reduced because a given dislocation possesses a limited capture radius correlated with the in-plane diffusion lengths of the charge carriers, ~500 nm in QD active regions[11]. Considering solely the number of dislocations per unit area and capture area per dislocation, one discovers that the total area influenced by dislocations decreases from 55% to 8% as the dislocation density drops from 7×10^7 cm^{-2} to 1×10^7 cm^{-2}. Going farther to our state-of-the-art buffers with 7×10^6 cm^{-2} TDD yields an affected area of 5% and comparing similar designs on GaAs, reveals essentially identical performance to the native substrate devices.

Unfortunately, while the gap in initial performance may be closed, large discrepancies arise during aging. As devices age under constant electrical bias, the dislocations in the material will grow through recombination enhanced climb and glide processes. While QDs are significantly more robust than QWs to such degradation, they are by no means immune, and extremely strong correlations between extrapolated time-to-failure and dislocation density have been observed[25]. At an elevated temperature of 80°C (as shown in Figure 4), devices on native substrate outperform our best material on silicon by approximately two orders of magnitude when defining failure as a doubling of the initial threshold current. The data points in Figure 4 represent best performing devices from larger datasets described in [25, 26]. In order to be viable for commercial applications such as those within datacenters and for high performance computing, lasers must be able to operate comfortably at temperatures >60°C with extrapolated lifetimes >100,000 h, and temperatures of 80-100°C will be necessary as lasers move closer to the CPU or get deployed for automotive LIDAR purposes. Currently, our lasers possess world record performance for reliability when grown on silicon, but they still fall short of meeting commercial metrics at temperatures >60°C, necessitating further investigation and reduction of the dislocation density as well as investigation of other aspects such as the residual tension in III-V/Si that results from the mismatch in thermal expansion coefficient. Furthermore, the fact that the native substrate lasers are only marginally acceptable at 80°C indicates that there are likely degradation mechanisms independent of the substrate also in play that should be addressed in our designs, perhaps relating to our deeply etched ridges and high stress dielectric cladding.

Downloaded From: https://www.spiedigitallibrary.org/conference-proceedings-of-spie on 13 May 2020
Terms of Use: https://www.spiedigitallibrary.org/terms-of-use

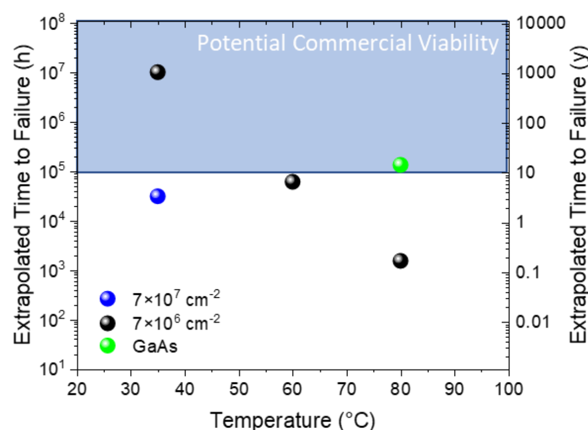

Figure 4. Extrapolated time-to-failure (defined as a doubling of the initial threshold current) is plotted as a function of aging temperature for devices aged at a bias of twice their initial threshold current density. Two levels of dislocation density are shown in addition to an identical epi structure grown on a native GaAs substrate. The 7×10^{7} cm^{-2} material corresponds to that shown in Figure 3 and contains seven dot layers while the other contain five dot layers and refers to Figure 2(c,f).

4. EPITAXIAL LASERS ON SILICON FOR PHOTONIC INTEGRATION

The significant recent progress in closing the performance gap between native and heteroepitaxial III-V/Si QD lasers has motivated more advanced studies in laser performance in preparation for photonic integration[27-29]. Particular emphasis has been placed in two areas that QD lasers have shown exemplary native substrate performance exceeding that achievable with QWs, namely feedback sensitivity[15, 30, 31] and low noise, narrow pulsewidth mode-locking[17, 32, 33]. Feedback sensitivity is critical to achieving an efficient, low noise light source in the presence of unintentional reflections from other integrated components. Meanwhile, mode-locked lasers represent the most efficient source of frequency comb generation making excellent candidates for simple, high integration density, efficient, and high-performance wavelength division multiplexing (WDM) systems for high bandwidth density. Recent studies have shown that the dynamic performance benefits provided by QDs on native substrates are readily extendable to silicon.

Sensitivity to optical feedback is primarily determined by the linewidth enhancement factor, α_H, and damping in the relaxation oscillation[34]. In QD lasers, ultralow linewidth enhancement factors are achievable and laser oscillations are overdamped[13, 30] which leads to remarkable insensitivity to external reflections[15]. Achieving these results requires extensive optimization of the QD growth conditions to minimize inhomogeneous broadening[16]. Table 1 summarizes the relative performance of first generation QD material grown on Si (Gen-I) with that of our third generation (Gen-III, corresponding to the reliability results above and buffer depicted in Figure 2(c,f)). Improvements in inhomogeneous broadening and TDD have resulted in a >4-fold reduction in α_H and the demonstration of operation with complete insensitivity to back-reflection levels up to 100% [15, 31]. In contrast, a commercially available C-band Fabry-Perot quantum well laser compared in the same study shows a 15-fold higher α_H and massively reduced critical feedback level of only 1.7% (-25 dB).

Downloaded From: https://www.spiedigitallibrary.org/conference-proceedings-of-spie on 13 May 2020
Terms of Use: https://www.spiedigitallibrary.org/terms-of-use

Table 1. A comparison of optical feedback characteristics for two generations of quantum dot epi material—referring to Figure 2(a,d) and (c,f)—with a commercial C-band quantum well is presented. The critical feedback level does not account for a 10% tap for measurement.

	Gen-I Quantum Dot	Gen-III Quantum Dot	Commercial C-band Quantum Well
Photoluminescence FWHM (meV)	54	30	N/A
Dislocation Density	3×10^{8} cm^{-2}	7×10^{6} cm^{-2}	Native Substrate
α_H	0.55	0.13	2.8
Critical Feedback Level	8%	>20%	0.3%

5. CONCLUSION

To summarize, quantum dot lasers grown on silicon show promise not only as an economic improvement to commercial photonic integration technology, but they also have demonstrated superior performance capabilities. The most significant remaining challenge is to demonstrate high temperature operation and reliability suitable for commercial applications. The current state-of-the-art performance levels show marginal acceptability at 60°C but require substantial improvements to achieve reliable operation at higher temperatures. Reducing the dislocation density remains the most obvious path forward, but additional work leveraging existing knowledge in native substrate semiconductor laser reliability will be required as well. The demonstration of feedback-insensitive operation will certainly drive adoption of QD lasers even on native substrates for the ability to eliminate optical isolation requirements in many applications, resulting in simplified packaging and photonic design requirements and potentially opening up new photonic integration implementations. Quantum dot lasers stand poised to transform the photonics industry over the coming years through simultaneously enabling significant cost reductions and performance improvements.

ACKNOWLEDGMENTS

The work was funded by the Advanced Research Projects Agency-Energy (ARPA-E), U.S. Department of Energy, under Award No. DE-AR0000843. The views and opinions of the authors expressed herein do not necessarily state or reflect those of the United States Government or any agency thereof.

REFERENCES

[1] Jones, R., Doussiere, P., Driscoll, J. B. *et al.*, "Heterogeneously Integrated InP\/Silicon Photonics: Fabricating Fully Functional Transceivers," IEEE Nanotechnology Magazine, 13(2), 17-26 (2019).

[2] Doerr, C. R., "Silicon photonic integration in telecommunications," Frontiers in Physics, 3, 37 (2015).

[3] Mudumba, S., de Alba, S., Romero, R. *et al.*, "Photonic ring resonance is a versatile platform for performing multiplex immunoassays in real time," Journal of immunological methods, 448, 34-43 (2017).

[4] Xie, W., Komljenovic, T., Huang, J. *et al.*, "Heterogeneous silicon photonics sensing for autonomous cars," Optics express, 27(3), 3642-3663 (2019).

[5] Shen, Y., Harris, N. C., Skirlo, S. *et al.*, "Deep learning with coherent nanophotonic circuits," Nature Photonics, 11(7), 441 (2017).

[6] Bunandar, D., Lentine, A., Lee, C. *et al.*, "Metropolitan quantum key distribution with silicon photonics," Physical Review X, 8(2), 021009 (2018).

[7] Liu, A. Y., and Bowers, J. E., "Photonic integration with epitaxial III-V on silicon," IEEE Journal of Selected Topics in Quantum Electronics, (2018).

Downloaded From: https://www.spiedigitallibrary.org/conference-proceedings-of-spie on 13 May 2020
Terms of Use: https://www.spiedigitallibrary.org/terms-of-use

[8] Tang, M., Chen, S., Wu, J. *et al.*, "Optimizations of defect filter layers for 1.3-μm InAs/GaAs quantum-dot lasers monolithically grown on Si substrates," IEEE Journal of Selected Topics in Quantum Electronics, 22(6), (2016).
[9] Jung, D., Callahan, P. G., Shin, B. *et al.*, "Low threading dislocation density GaAs growth on on-axis GaP/Si (001)," Journal of Applied Physics, 122(22), 225703 (2017).
[10] Liu, A. Y., Srinivasan, S., Norman, J. *et al.*, "Quantum dot lasers for silicon photonics," Photonics Research, 3(5), B1-B9 (2015).
[11] Selvidge, J., Norman, J., Salmon, M. E. *et al.*, "Non-radiative recombination at dislocations in InAs quantum dots grown on silicon," Applied Physics Letters, 115(13), 131102 (2019).
[12] Liu, Z., Hantschmann, C., Tang, M. *et al.*, "Origin of defect tolerance in InAs/GaAs quantum dot lasers grown on silicon," Journal of Lightwave Technology, (2019).
[13] Norman, J. C., Jung, D., Zhang, Z. *et al.*, "A Review of High-Performance Quantum Dot Lasers on Silicon," IEEE Journal of Quantum Electronics, 55(2), 1-11 (2019).
[14] Kageyama, T., Nishi, K., Yamaguchi, M. *et al.*, "Extremely high temperature (220° C) continuous-wave operation of 1300-nm-range quantum-dot lasers." PDA_1.
[15] Duan, J., Huang, H., Dong, B. *et al.*, "1.3-μm Reflection Insensitive InAs/GaAs Quantum Dot Lasers Directly Grown on Silicon," IEEE Photonics Technology Letters, 31(5), 345-348 (2019).
[16] Zhang, Z., Jung, D., Norman, J. *et al.*, "Linewidth enhancement factor in InAs/GaAs quantum dot lasers and its implication in isolator-free and narrow linewidth applications," IEEE Journal of Selected Topics in Quantum Electronics, (2019).
[17] Liu, S., Wu, X., Jung, D. *et al.*, "High-channel-count 20 GHz passively mode-locked quantum dot laser directly grown on Si with 4.1 Tbit/s transmission capacity," Optica, 6(2), 128-134 (2019).
[18] Liu, S., Norman, J., Dumont, M. *et al.*, "High-Performance O-band Quantum-Dot Semiconductor Optical Amplifiers Directly Grown on a CMOS Compatible Silicon Substrate," ACS Photonics, (2019).
[19] Li, Q., Ng, K. W., and Lau, K. M., "Growing antiphase-domain-free GaAs thin films out of highly ordered planar nanowire arrays on exact (001) silicon," Applied Physics Letters, 106(7), 072105 (2015).
[20] Németh, I., Kunert, B., Stolz, W. *et al.*, "Heteroepitaxy of GaP on Si: Correlation of morphology, anti-phase-domain structure and MOVPE growth conditions," Journal of Crystal Growth, 310(7-9), 1595-1601 (2008).
[21] Shchukin, V., Ledentsov, N. N., and Bimberg, D., [Epitaxy of nanostructures] Springer Science & Business Media, (2013).
[22] Nishi, K., Takemasa, K., Sugawara, M. *et al.*, "Development of quantum dot lasers for data-com and silicon photonics applications," IEEE Journal of Selected Topics in Quantum Electronics, 23(6), 1-7 (2017).
[23] Ozdemir, S., Suyolcu, Y. E., Turan, S. *et al.*, "Influence of the growth conditions on the optical and structural properties of self-assembled InAs/GaAs quantum dots for low As/In ratio," Applied Surface Science, 392, 817-825 (2017).
[24] Norman, J., [Quantum Dot Lasers for Silicon Photonics] UC Santa Barbara, (2018).
[25] Jung, D., Herrick, R., Norman, J. *et al.*, "Impact of threading dislocation density on the lifetime of InAs quantum dot lasers on Si," Applied Physics Letters, 112(15), 153507 (2018).
[26] Norman, J., Zhang, Z., Jung, D. *et al.*, "The Importance of p-Doping for Quantum Dot Laser on Silicon Performance," IEEE Journal of Quantum Electronics, In Press (2019).
[27] Hantschmann, C., Vasil'ev, P. P., Chen, S. *et al.*, "Gain switching of monolithic 1.3 μm InAs/GaAs quantum dot lasers on silicon," Journal of Lightwave Technology, 36(18), 3837-3842 (2018).
[28] Hantschmann, C., Vasil'ev, P. P., Wonfor, A. *et al.*, "Understanding the bandwidth limitations in monolithic 1.3 μm InAs/GaAs quantum dot lasers on silicon," Journal of Lightwave Technology, 37(3), 949-955 (2018).
[29] Inoue, D., Jung, D., Norman, J. *et al.*, "Directly modulated 1.3 μm quantum dot lasers epitaxially grown on silicon," Optics express, 26(6), 7022-7033 (2018).
[30] Duan, J., Huang, H., Jung, D. *et al.*, "Semiconductor quantum dot lasers epitaxially grown on silicon with low linewidth enhancement factor," Applied Physics Letters, 112(25), 251111 (2018).
[31] Huang, H., Duan, J., Jung, D. *et al.*, "Analysis of the optical feedback dynamics in InAs/GaAs quantum dot lasers directly grown on silicon," JOSA B, 35(11), 2780-2787 (2018).
[32] Auth, D., Liu, S., Norman, J. *et al.*, "Passively mode-locked semiconductor quantum dot on silicon laser with 400 Hz RF line width," Optics Express, 27(19), 27256-27266 (2019).
[33] Liu, S., Jung, D., Norman, J. *et al.*, "490 fs pulse generation from passively mode-locked single section quantum dot laser directly grown on on-axis GaP/Si," Electronics Letters, 54(7), 432-433 (2018).

Downloaded From: https://www.spiedigitallibrary.org/conference-proceedings-of-spie on 13 May 2020
Terms of Use: https://www.spiedigitallibrary.org/terms-of-use

[34] Coldren, L. A., Corzine, S. W., and Mashanovitch, M. L., [Diode lasers and photonic integrated circuits] John Wiley & Sons, (2012).

Downloaded From: https://www.spiedigitallibrary.org/conference-proceedings-of-spie on 13 May 2020
Terms of Use: https://www.spiedigitallibrary.org/terms-of-use